Design and Implementation of a Li-ion Battery Charger from a Solar Panel

Eduardo Rodríguez Mejía, Rafel F. Díez Medina, *Member, IEEE* and Gabriel Perilla Galindo, *Member, IEEE*

***Abstract*—The following article shows the design and implementation of a battery charger for Li-ion batteries with a capacity of 48 V at 25 Ah from a solar panel of at least 200 Wp. The implementation will include a Perturb and Observe (P&O) Maximum Power Point Tracker algorithm (MPPT) for the Constant Current (C.C.) stage and a PI controller for the Constant Voltage (C.V.) stage. In section II the converter characteristics will be presented, and equations will be derived alongside circuit model, section III will account for the P&O algorithm and PI controller implementation in a Microcontroller Unit (MCU) and section IV will show the general control system implementation with a Finite State Machine (FSM). Finally, section V holds up the results and section VI will include conclusions and future work.**

***Index Terms*—Battery chargers, Lithium batteries, Microcontrollers, Solar power generation.**

I. Introduction

Aiming for a better efficiency and reliability of electricity distribution service, use and integration of different technologies, like solar panels and high capacity batteries, appears as an alternative in energy converting systems for grid connected consumers. This kind of systems will have to account for maximum generation while integrating devices that help measure different electrical variables that allow decision making regarding the management of the energy production. In short, these systems will have to ensure energy availability at any required moment, with the appropriate tension levels for consumption within the household or for grid feeding.

For the grid connected system, it will be necessary to manage the power delivery according to the necessity of the household, borrowing energy from the grid, to charge the batteries or supply energy for consumption, or feeding the excess stored energy to the grid for its usage where it is more needed. As for the solar power generation backup system, it will need to maximize energy production during the day to help maintain battery charge state and reduce the need of buying energy from the grid. The following article will be center in the solar powered backup system.

II. Converter Characteristics and Circuit Model

The DC-DC charge controller converter input source will be a 285 Wp PV panel [1] with a voltage between 15 V and 31.7 V and an input current between 2.0 A and 8.89 A, for irradiances from 200 W/m^2 to 1000 W/m^2. The load of this converter is a 48 V Li-ion battery rated for 25 Ah [2] with a voltage range from 40 V to 58.4 V and with a maximum charge current of 25 A. From these requirements a Ćuk converter topology is selected as the core DC/DC converter for this approach because offers and input and output filter that will assure continuous average current being drawn from the panel and feed to the battery.

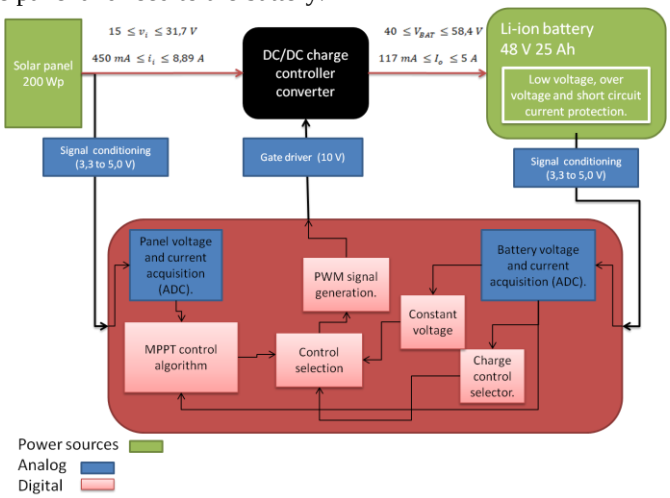

Fig. 1. General system block diagram.

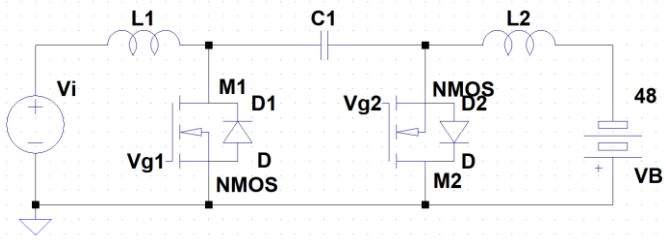

Fig. 2. Ćuk converter topology.

A. Circuit behavior

Figures 3 and 4 shown the equivalent circuit for each conduction interval, $D.T$ and $(1-D).T$, with the ideal circuit elements and the corresponding equations for each energy storage element.

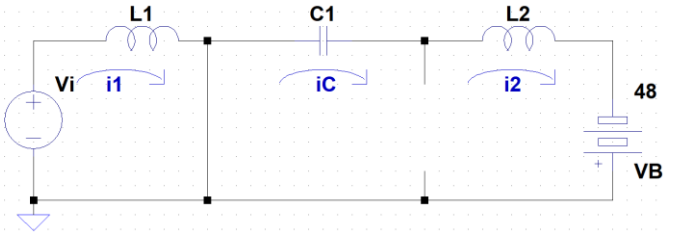

Fig. 3. Equivalent circuit at $D.T$

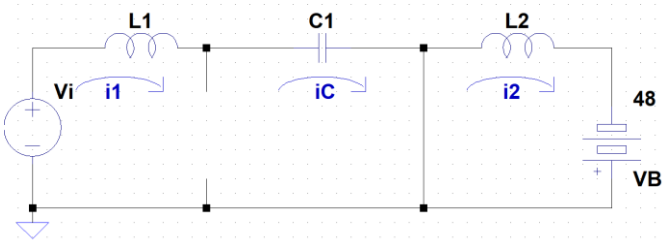

Fig. 4. Equivalent circuit at $(1-D).T$

For the first interval, when M1 in on and M2 off (D), the following equations can be obtained from the volt-second balance in L1 and L2 and charge balance in C1:

$$v_{L1} = V_i - i_1.R_{L1} - (i_1 - i_c).r_{dson1}$$

$$v_{L2} = (i_1 - i_c).r_{dson1} - i_c.ESR_1 - V_{C1} - i_2.R_{L2} + V_o$$

$$i_{C1} = i_2$$

$$i_2 = -I_O$$

At second interval, when M1 is off and M2 on $(1-D)$, the following is true:

$$v_{L1} = V_i - i_1.R_{L1} - i_c.ESR_1 - V_{C1} - (i_c - i_2).r_{dson2}$$

$$v_{L2} = (i_c - i_2).r_{dson2} - i_2.R_{L2} + V_o$$

$$i_{C1} = i_1$$

$$i_2 = -I_O$$

Unifying the equations for both intervals we obtain

$$v_{L1} = V_i - i_1.R_{L1} - (i_1 - i_2).r_{dson1}.D \\ -(i_1 - i_2).r_{dson2}.(1-D) - i_1.ESR_1.(1-D) - V_{C1}.(1-D)$$

$$v_{L2} = -i_2.R_{L2} + (i_1 - i_2).r_{dson1}.D \\ + (i_1 - i_2).r_{dson2}.(1-D) - i_2.ESR_1.D \\ - V_{C1}.D + V_O$$

$$i_{C1} = i_2.D + i_1.(1-D)$$

$$i_2 = -I_O$$

Where one can obtain the general expressions for voltage and current

$$V_O = \frac{-V_i.D}{(1-D)}$$

$$V_{C1} = \frac{V_i}{(1-D)}$$

$$i_1 = \frac{-I_O.D}{(1-D)}$$

B. *Circuit model*

For circuit AC modelling the previous equations are recreated in *Simulink* alongside circuit simulation. Transfer function equations are obtained for each variable of energy storage elements and output voltage.

$$\frac{i_{L1}}{d} = \frac{1{,}983 * 10^5.s^2 + 2{,}534 * 10^8.s - 3{,}094 * 10^{13}}{s^3 + 173{,}2.s^2 + 1{,}415 * 10^8.s + 1{,}803 * 10^{10}}$$

$$\frac{i_{L2}}{d} = \frac{-1{,}983 * 10^5.s^2 + 2{,}997 * 10^8.s - 2{,}446 * 10^{13}}{s^3 + 173{,}2.s^2 + 1{,}415 * 10^8.s + 1{,}803 * 10^{10}}$$

$$\frac{v_C}{d} = \frac{-1{,}98 * 10^5.s^2 - 2{,}33 * 10^9.s - 1{,}037 * 10^{11}}{s^3 + 173{,}2.s^2 + 1{,}415 * 10^8.s + 1{,}803 * 10^{10}}$$

$$\frac{v_o}{d} = \frac{-9{,}015 * 10^9.s^2 + 2{,}14 * 10^{13}.s - 1{,}081 * 10^{18}}{s^4 + 7620.s^3 + 1{,}534 * 10^8.s^2 + 9{,}761 * 10^{11} + 9{,}479 * 10^{14}}$$

III. DIGITAL IMPLEMENTATION

A. *P&O algorithm*

Figure 5 shows P&O algorithm flow chart that will be implemented in the MCU.

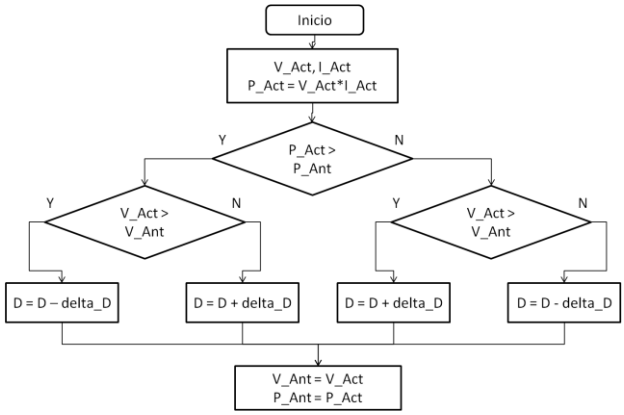

Fig. 5. P&O algorithm flow chart.

Input voltage and current are obtained and adequate to a maximum of 3.3 V for the ADC to convert, these values are multiply in the MCU for the input power value and finally compared with definitions for the critical cases as shown in figure 6.

```
if(P_P > P_Ant){
    if((V_P > V_Ant) && (D > D_Min)){
        D -= Delta_D;
    }
    else if(D < D_Max){
        D += Delta_D;
    }
}
else{
    if((V_P > V_Ant) && (D < D_Max)){
        D += Delta_D;
    }
    else if(D > D_Min){
        D -= Delta_D;
    }
}
```

Fig. 6. P&O algorithm implementation.

B. *PI controller*

From $\frac{v_o}{d}$ transfer function the PI controller is design with as follows:

$$PI(s) = \frac{-2{,}2957.(1 + 640 * 10^{-6}.s)}{s}$$

For digital implementation, it needs to be represented in terms of Z and rearrange into a difference equation.

$$PI(Z) = \frac{1{,}423 \times 10^{-3} - 1{,}469 \times 10^{-3}.Z}{Z - 1}$$

Figure 8 shows the behavior of the discrete controller in the circuit simulation as can be seen in figure 7.

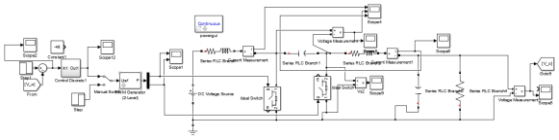

Fig. 7. Closed loop circuit simulation.

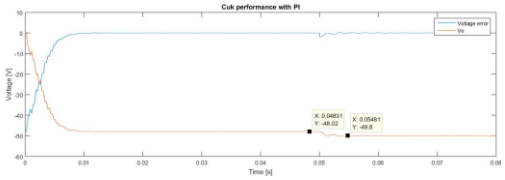

Fig. 8. Error and output voltage signal with PI controller.

Finally, figure 9 account for the digital implementation of the difference equation.

```
V_Err = V_Bat_Max - V_Bat;
V_D = V_D_Ant + V_Err*Kp + V_Err_Ant*Ki;
if(V_D >= V_D_Max){
    D = D_Max;
}
else if(V_D <= V_D_Min){
    D = D_Min;
}
else if((V_D > V_D_Min) || (V_D < V_D_Max)){
    D = (V_D*1000.0)/3.3;
}

V_Err_Ant = V_Err;
V_D_Ant = V_D;
```

Fig. 9. PI implementation.

IV. GENERAL CONTROL SYSTEM

At figure 10, the FSM for general control system is presented. The purpose of this implementation is to maintain MPPT as long as the battery is under its nominal charge value and there is enough input power. Given the case that the battery is completely charge during the day, it will switch to C.V. state and maintain while the battery is at full charge.

Comparación V_P is the state for checking is there is enough radiation, given the fact that the converter should be off and solar panel voltage will be the equivalent of the open circuit value, *PWM_ON* is for starting the control signals for each transistor, and *PWM_OFF* for stopping the signals when the input power falls to much.

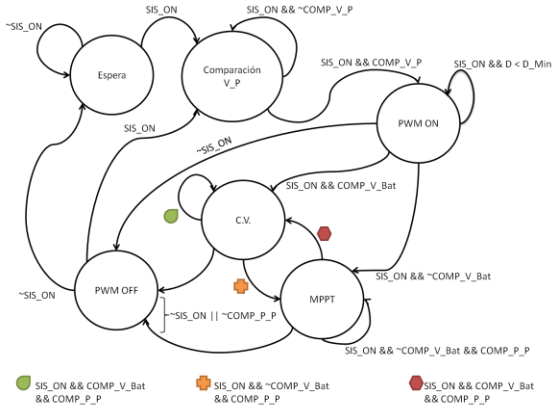

Fig. 10. General control system FSM.

Digital implementation of the FMS is done with as a function with a switch-case code, where each state is a case that holds the corresponding action and if-else statements to make the transitions from one state to another.

V. RESULTS

A. *MPPT algorithm*

Oscilloscope screen capture of figure 11 shown system behavior at MPPP state and figure 12 shows behavior for different irradiances.

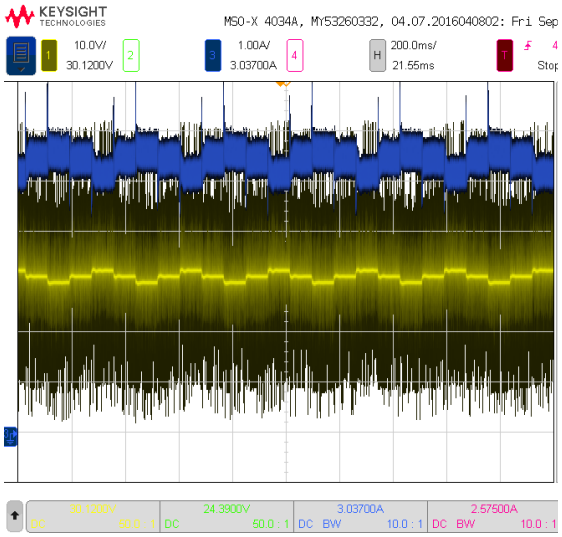

Fig. 11. Input voltage in yellow and input current in blue for converter at MPPT state.

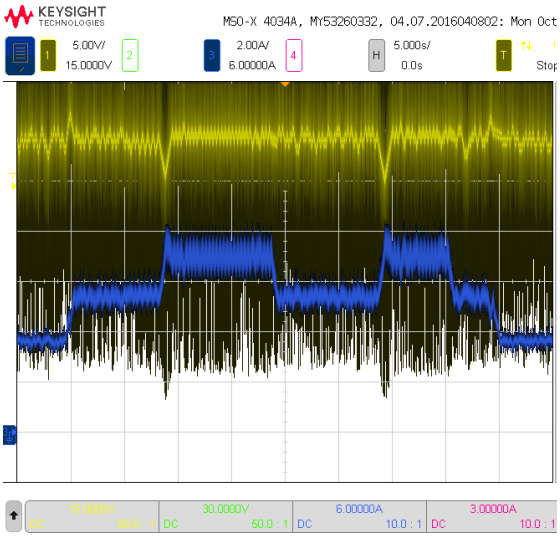

Fig. 12. Input voltage in yellow and input current in blue for converter at different irradiance values at MPPT state.

B. PI controller

Figure 13 shows system behavior with a change from MPPT state to C.V. state for input voltage and current.

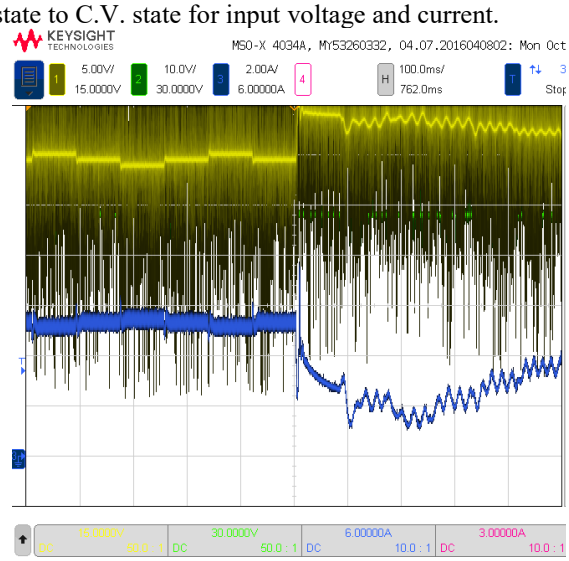

Fig. 13. Input voltage in yellow and input current in blue for converter when transitioning from MPPT to C.V. state.

VI. Conclusion and Future Work

Ćuk converter final implementation is shown in figures 14 and 15, figure 14 shows power stage with corresponding sensor and supply voltages and figure 14 includes the digital circuit board with the MCU development board, ADC input channels and PWM control signals.

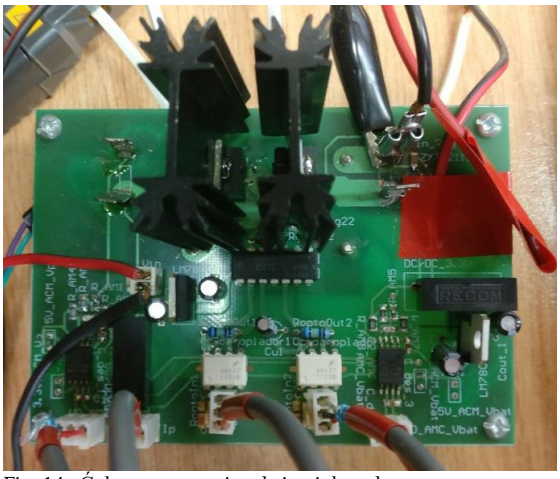

Fig. 14. Ćuk converter printed circuit board.

Fig. 14. Ćuk converter and digital control printed circuit board.

P&O algorithm is the easiest one for an implementation, requiring only a voltage and current sensor for obtaining the input power and comparing it with the last acquired value, but it also is the less accurate when comparing it to others like incremental conductance, method that requires to obtain the derivate of the power at each acquired point to know if the slope is positive, negative or cero, determining the required action for the duty cycle.

Because of the system restrictions, the current sensor for the output is not needed, reducing size and eliminating the control loop. As long as the battery is discharge, MPPT will assure maximum charging current is being feed to the battery.

As for the digital implementation, the system maximum overhead during MPPT state is around 100 ms for just 1 battery charging system, making it plausible to use 1 MCU for a series of systems within a pooling loop structure where the ADC input channels are multiplexed for each system and the corresponding PWM signals are updated accordingly to the processing in each of the system FSM functions.

For future work, the charging systems will have to work along a multilevel inverter that will have its input to 5 batteries and will acts as a bidirectional system to charge it from the grid or supply energy to it. Because the 5 batteries will supply energy to the inverter circuit, the solar power generation system will charge one battery only, meaning that when one of

them is fully charge and there is still enough input power, the system will loss its potential. As an alternative, output inductances of the 5 required systems will need to be couple, so that the systems will charge all of the batteries according to the lowest level one to the highest until all of them reach floating voltage, increasing the system efficiency and optimizing energy production from the solar panels. For this, printed circuit boards will need to be redesigned for holding the coupled inductors and possibly increasing the output trace width for managing more current at the output.

REFERENCES

[1] V. A. Boicea, «Energy Storage Technologies: The Past and the Present,» *IEEE xplore,* vol. 102, nº 11, pp. 1777-1794, 2014.

[2] REN21, «RENEWABLES 2018 GLOBAL STATUS REPORT,» París, 2018.

[3] V. Aggarwal, «What are the most efficient solar panels on the market?,» 2 Junio 2018. [En línea]. Available: https://news.energysage.com/what-are-the-most-efficient-solar-panels-on-the-market/. [Último acceso: 27 Junio 2018].

[4] R. W. Erickson, Fundamentals of Power Electronics, Nueva York: Kluver Academic, 2004.

[5] Canadian Solar, «CanadianSolar CS6K- 275 |280 |285 M,» Ontario, 2016.

[6] Smart Battery, «48V 25AH Deep Cycle Lithium Ion Battery,» [En línea]. Available: http://www.lithiumion-batteries.com/products/48-volt-lithium-batteries/48v-25ah-deep-cycle-lithium-ion-battery.php. [Último acceso: 14 Febrero 2017].

[7] Woodbank Communications Ltd, «Battery Chargers and Charging Methods,» Battery and Energy Technologies, 2005. [En línea]. Available: http://www.mpoweruk.com/chargers.htm. [Último acceso: 02 Octubre 2017].

[8] Battery University, «Battery University,» [En línea]. Available: http://batteryuniversity.com/learn/article/charging_lithium_ion_batteries. [Último acceso: 2 Octubre 2017].

[9] Ferroxcube, «Soft ferrites and accesories Data handbook,» pp. 36,124,563-564, 2013.

[10] A. R. H. R. N. R. F. Rasoul Faraji, «FPGA-based real time incremental conductance maximum power point tracking controller for photovoltaic systems,» *IET Power Electronics*, p. 1294–1304, 2013.

[11] T. P. Sahu y T. V. Dixit, «Modelling and Analysis of Perturb & Observe and Incremental Conductance MPPT Algorithm for PV Array Using Cuk Converter,» *2014 IEEE Student's Conference on Electrical, Electronics and Computer Science*, pp. 1-6, 2014.

[12] D. M. ALVAREZ MENESES, «CONVERTIDOR DC/DC PARA CARGA DE BATERÍAS DE BAJO VOLTAJE DE ALMACENAMIENTO PARA SISTEMA FOTOVOLTAICO,» Bogotá, 2017.

[13] A. Wiesner, D. Rafael y P. Gabriel, «Energy Storage System from DC Bus with Port for Solar Module,» *IEEE LATIN AMERICA TRANSACTIONS*, vol. 13, nº 5, pp. 1376-1382, 2015.

[14] D. R. C. Nayar, «Analysis and Design of a Solar Charge Controller Using Cuk Converter».

[15] S. Armstrong, M. Glavin y W. Hurley, «Comparison of Battery Charging Algorithms for Stand Alone Photovoltaic Systems,» *IEEE Xplore*, pp. 1469-1475, 2008.

[16] Canadian Solar, «CS6K- 275 |280 |285 M,» Ontario.

[17] IDEAM, «Atlas de Radiación Solar, Ultravioleta y Ozono de Colombia,» [En línea]. Available: http://atlas.ideam.gov.co/visorAtlasRadiacion.html. [Último acceso: 14 Febrero 2017].

[18] A. Wiesner, D. Rafael y P. Gabriel, «Design and implementation of a Buck converter with MPPT for battery charge from solar module.,» *IEEE xplore*, 2013.

[19] M. G. W. H. S. Armstrong, «Comparison of Battery Charging Algorithms for Stand Alone Photovoltaic Systems,» *IEEE xplore*, pp. 1469-1475, 2008.

[20] S. A. Pérez P., Estudio de diferentes topologías para interconexión a la red de fuentes renovables, Bogotá, 2016.

[21] R. V. Jain, M. V. Aware y A. S. Junghare, «Implementation of a PID control PWM Module on Altera DE0 Kit Using FPGA,» *Ieee xplore*, pp. 341-345, 2016.

[22] A. R. H. R. N. R. F. R. C. Rasoul Faraji, «FPGA-based real time incremental conductance maximum power point tracking controller for photovoltaic systems,» *IET Power Electronics*, vol. 7, p. 1294–1304, 2014.